Available online at www.sciencedirect.com

ScienceDirect

Geochimica et Cosmochimica Acta 294 (2021) 1–12

Geochimica et Cosmochimica Acta

www.elsevier.com/locate/gca

A model of algal organic carbon distributions in the Pearl River estuary using the amino acid carbon isotope values

Peihong Kang [a,b], Han Zhang [c], Zixiang Yang [a,b], Yifan Zhu [a,b], Biyan He [d], Qing Li [a,b], Cindy Lee [e], Tiantian Tang [a,b,*]

[a] State Key Laboratory of Marine Environmental Science (Xiamen University), Xiamen, Fujian 361102, China
[b] College of Ocean and Earth Sciences, Xiamen University, Xiamen, Fujian 361102, China
[c] Key Laboratory of Urban Environment and Health, Institute of Urban Environment, Chinese Academy of Sciences, Xiamen, Fujian 361021, China
[d] College of Harbour and Environmental Engineering, Jimei University, Xiamen, Fujian 361021, China
[e] School of Marine and Atmospheric Sciences, Stony Brook University, Stony Brook, NY 11794-5000, United States

Received 8 May 2020; accepted in revised form 11 November 2020; available online 20 November 2020

Abstract

To better understand the sources and behavior of estuarine labile organic matter, we measured stable carbon isotope patterns of individual amino acids in suspended particles and surface sediments from the Pearl River Estuary in China; samples were taken along a salinity transect in December, 2016. Here we demonstrate that carbon isotope values ($\delta^{13}C$) of individual amino acids in these samples gradually increase with salinity downstream, reflecting the increase in $\delta^{13}C$ values of algal-derived organic carbon along the salinity gradient. The isotopic difference between amino acids and bulk organic carbon varies, most likely due to changes in the relative contributions of algal-derived organic matter and refractory terrestrial input. In addition, algal-derived organic matter can consist of labile and semi-labile organic matter in varied proportions depending on degradation state. This isotopic difference between amino acids and bulk organic carbon is much larger in surface sediments than in suspended particles, suggesting that labile organic carbon contributed more to suspended particles than to sediments. Using the relative abundances and $\delta^{13}C$ ratios of amino acids and total organic carbon, a Lability Model was constructed to evaluate the relative contributions of three forms of estuarine organic carbon: labile algal material as amino acids, semi-labile algal material as lipids and acid-insoluble material, and refractory terrestrial organic material. The model suggests highly dynamic contributions of semi-labile algal-derived organic carbon and terrestrial organic carbon to estuarine particulate organic carbon. This evaluation of organic carbon sources illustrates the importance of decomposition in shaping the molecular composition and isotopic signature of particulate organic carbon in the estuary.

Keywords: Amino acids; Compound specific isotope analysis (CSIA); Pearl River estuary; South China Sea; Phytoplankton; Labile organic matter; Sediment organic matter; Particulate organic matter

1. INTRODUCTION

Carbon isotope values ($\delta^{13}C$) of algal cells are determined by two factors, the inorganic carbon source of the cell and the isotopic fractionation during carbon fixation (Rau et al., 1992; Popp et al., 1998). Although they share the same carbon source, individual compounds within the

* Corresponding author at: State Key Laboratory of Marine Environmental Science (Xiamen University), Xiamen, Fujian 361102, China.
E-mail address: tiantian.tang@xmu.edu.cn (T. Tang).

https://doi.org/10.1016/j.gca.2020.11.010
0016-7037/

cell have different $\delta^{13}C$ values due to differing extents of fractionation during the various metabolic pathways used to synthesize these compounds (Degens et al., 1968; DeNiro and Epstein, 1977; Wilkes et al., 2017, 2018). Thus, the $\delta^{13}C$ value of bulk organic carbon depends on the relative composition and $\delta^{13}C$ of all the individual compounds (Hayes, 2001). Among the individual organic compound classes in algae, amino acids and carbohydrates have slightly higher $\delta^{13}C$ values relative to bulk organic carbon, while lipids are generally lower in ^{13}C relative to the bulk (Hayes, 2001; Close, 2019). The molecular composition of algal materials changes over time as the algae decompose (Wakeham and Lee, 2019). In the equatorial Pacific, for example, amino acids account for 67% of net plankton, while in the deep water, most of those amino acids have been either transformed or preferentially removed, leaving most of the organic matter (OM) molecularly uncharacterized (Wakeham et al.,1997; Hedges et al., 2000; Hwang et al., 2006). The isotopic signature of one part of this uncharacterized material has been investigated as the 'acid-insoluble fraction' (AIF, Wang et al., 1998; Hwang and Druffel, 2003; Roland et al., 2008). AIF is an operational definition referring to the OM fraction that cannot be extracted by acid or organic solvent. The AIF is assumed to be a refractory component of biological origin (Hedges et al., 2000; Hwang et al., 2006) that shares similar carbon isotope values to lipids, generally 4.53‰ lower in ^{13}C than total hydrolyzable amino acids (Hwang and Druffel, 2003). Meanwhile, organic compounds vary in their lability, i.e., their tendency to be decomposed. Under the same environmental conditions, refractory OM like AIF will have a slower decomposition rate than more labile OM like amino acids. As a result, a decrease of bulk organic carbon $\delta^{13}C$ can be observed as organic matter decomposes, due to more labile compounds being lost and AIF increasing in relative abundance (Jeffrey et al., 1983; Wang et al., 1998).

The production of algal-derived OM can be high in estuaries where there is an abundant supply of nutrients (Canuel et al., 1995; Qian et al., 1996; Canuel and Hardison, 2016). Terrestrial plant debris and soil OM can also be sources of organic matter to estuaries. Particulate OM in estuaries is a combination of various amounts of all three sources and depends on location (Bianchi and Bauer, 2011). Algal-derived OM is dominated by rather labile OM like amino acids, carbohydrate and lipids; for example, amino acids account for 20–50% of algal carbon compared to <5% amino acids in terrestrial vascular plants (Whitehead et al., 2008, Canuel and Hardison, 2016). Therefore, algal-derived OM is usually subject to more rapid decomposition in estuaries compared to more recalcitrant terrestrial OM from soil OM or vascular plants (Mannino and Harvey, 1999; McCallister et al., 2006; McIntosh et al., 2015). These changes in molecular composition due to degradation alter the lability of estuarine OM and hence the fate of compounds that are exported to the ocean (Hedges et al., 1997). Quantifying the effect of degradation on OM is particularly challenging in estuarine systems where highly labile algal-derived OM and more recalcitrant terrestrial OM are both present (Roland et al., 2008; Canuel and Hardison, 2016). Thus, quantitative evaluation of the fate of organic carbon in the estuary and its export to the ocean has large uncertainties (Hedges et al., 1997).

Differences in bulk organic carbon $\delta^{13}C$ values are frequently observed in estuaries, with lower $\delta^{13}C$ OM at the river end than at the ocean end (Peterson and Fry, 1987). This isotopic difference has been widely applied using two-end member mixing models to indicate terrestrial vs. marine origin of organic matter (Bianchi and Bauer, 2011 and the reference therein). A three-end member model combining bulk organic carbon $\delta^{13}C$ values with molecular composition information (e.g., lignin content) can improve the differentiation of organic carbon into soil OM, terrestrial plant OM, and marine OM (Goñi et al., 1998; Gordon and Goni, 2003; Zhang et al., 2014; Li et al., 2014; Yao et al., 2015). However, the application of this type of model is frequently limited due to the complicated sources of estuarine organic matter having overlapping isotope values (Cloern et al., 2002). Moreover, organic matter from different sources can have different molecular compositions and labilities so that the extent of OM transformation also varies in the estuary (Mannino and Harvey, 1999; McCallister et al., 2006; Bianchi, 2011).

Carbon isotope values of individual compounds can provide detailed information on the source and transformation of estuarine organic matter (Qian et al., 1996; Hedges et al., 1997; McIntosh et al., 2015; Canuel and Hardison, 2016). Distinctive carbon isotope values of amino acids have been identified among major domains of organisms (Scott et al., 2006; Larsen et al., 2009, 2012, 2013; Tang et al., 2017). The carbon isotope values of individual amino acids in both marine and fresh water environments have been used to identify the metabolic origin of labile organic matter in sediments (Keil and Fogel, 2001; Larsen et al., 2015), sinking particles (McCarthy et al., 2004), and suspended particles (Hannides et al., 2013; Sabadel et al., 2019). An investigation of amino acid carbon isotope values in sediment OM and phytoplankton in the Columbia River Estuary shows how amino acid isotopic values were determined by their OM sources and by microbial reworking (Keil and Fogel, 2001).

This preliminary study investigated the contribution of algal-derived OM and its degradative products in the Pearl River estuary using a Lability Model based on the carbon isotope values of amino acids. In this model, the organic matter in suspended particles was assumed to consist of 1) labile algal material (LabiAM) as amino acids, 2) semi-labile algal material (SemiAM) as lipids and acid-insoluble material (AIF) from algae, and 3) refractory terrestrial organic material (TerrOM). We assumed that the carbon isotope values of bulk particulate organic carbon (POC) reflect the relative abundance of these three groups of OM and their characteristic carbon isotopic values. Using the model, we then quantified the distribution of these three forms of organic carbon in the estuary, and characterized the relative lability of algal-derived organic matter specifically. The application of this model provides a novel approach to evaluate the contribution of algal organic matter and its degradational transformation to particulate organic carbon in estuaries.

2. MATERIALS AND METHODS

2.1. Sampling area

The Pearl River is the second largest river in China. Pearl River water discharge shows significant seasonality as a result of the East Asia Monsoon. This results in a longer residence time for water discharge and a characteristic salt wedge in the winter dry season (Dai et al., 2014). The most populated area in South China is located at the upper reaches of the Pearl River estuary (Fig. 1). After a number of reservoirs and dams were built in the Pearl River basin in the 1990s, the sediment load and suspended particulate matter concentrations in the estuary decreased greatly (Dai et al., 2008a; Zhang et al., 2008). Due to constrained physical mixing and increased anthropogenic nutrient inputs from industrial and agricultural activities, phytoplankton production has become the major source of organic matter to this estuary (Chen et al., 2004; Guo et al., 2015; Zhang et al., 2014), and this biodegradable organic matter experiences extensive consumption and diagenetic alteration during transport in the estuary (He et al., 2010a,b; Li et al., 2018).

2.2. Sample collection and analysis of chlorophyll *a* and nitrate

Suspended particle samples were collected along a transect down the Pearl River estuary (Fig. 1) on board the R/V Haishun in December 2016. Water was collected from 1 to 2 m below the surface using Niskin bottles, and immediately filtered onto separate precombusted 0.7-μm GF/F filters for analysis of chlorophyll, total suspended material (TSM), isotopes of individual amino acids, and isotopes of total organic carbon. Water was also immediately filtered through 0.4-μm polycarbonate filters for measurement of nitrate (NO_3^-) concentrations. All samples were stored at −20 °C until analysis. In the lab, chlorophyll *a* (Chl*a*) was extracted with methanol in the dark, and fluorescence of the extract was measured using a Turner fluorometer (Strickland and Parsons, 1972). NO_3^- concentrations were measured colorimetrically using an AA3 Auto-Analyzer (Technicon, Bran-Lube) (Dai et al., 2008b). TSM was calculated by weighing the dried particles on the GF/F filters.

Surface sediment samples were collected by scraping the top centimeters from a box core and then stored at −20 °C. They were later freeze-dried in the lab and sieved through a 65-μm mesh before amino acid and organic carbon isotopic analysis.

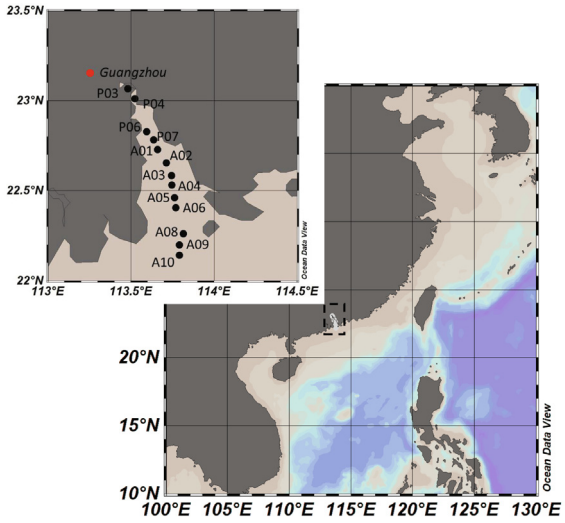

Fig. 1. Location of sampling sites along the Pearl River Estuary in December 2016 is shown in the zoomed inset of the dashed area in the larger map of the South China Sea and adjacent East Asia continent. Particle samples were collected at 9 stations, P04, P07, A01, A02, A04, A05, A06, A08 and A10, and sediment samples were collected at 5 stations, P03, P06, A03, A06, and A09. (Produced using Ocean Data View version 4.7.9).

2.3. Bulk organic carbon and bulk $\delta^{13}C$

Inorganic carbon was removed from filtered samples and sediments by acidification with a few drops of 1 N HCl, then dried overnight at 60 °C (Kao et al., 2012). Acidified filters and sediments were analyzed by elemental analyzer (EA)-isotope ratio mass spectrometry (IRMS, Isoprime 500). The organic carbon concentrations and $\delta^{13}C$ values were calibrated using glutamic acid (USGS-40) and acetanilide (Merck) standards. The analytical relative standard deviation (RSD) was 1.1% for the isotopic analysis and 2.5% for the bulk carbon concentrations.

2.4. Compound specific $\delta^{13}C$ analysis - amino acids

Particulate amino acids (PAA) and sediment amino acids (SAA) were released from samples by hydrolysis with HCl and then derivatized using a modification of Silfer et al. (1991) as described in Tang et al. (2017) (see Supplementary Materials S1.1). Amino acid derivatives were separated on a gas chromatography column (60 m × 0.25 mm, 0.25 μm, HP-5MS, Fig. S1), and carbon isotope ratios of individual amino acids were measured by coupled isotope ratio mass spectrometry (GC-C-IRMS, Thermo Delta V Advantage isotope ratio mass spectrometer coupled with a Trace GC via GC Isolink interface). Norleucine (Sigma-Aldrich) was added before hydrolysis as an internal standard. To correct isotopic values of the derivatized amino acids, an external standard of amino acids (Sigma-Aldrich) with known $\delta^{13}C$ values calibrated by EA-IRMS was prepared in parallel; this standard included alanine (Ala), glycine (Gly), threonine (Thr), leucine (Leu), valine (Val), isoleucine (Ile), proline (Pro), aspartic acid + asparagine (Asx), glutamic acid + glutamine (Glx), and phenylalanine (Phe), together with the internal standard norleucine.

Duplicates or triplicates of particle and sediment extracts were analyzed; standard deviations ranged from 0.0‰ to 4.3‰ among individual amino acids, and the average standard deviation ranged from 0.1‰ to 1.5‰ for averaged amino acids. The concentrations of individual amino acids were calibrated by comparing the peak area of CO_2 of samples and internal standard norleucine with the

external mixed amino acid standard. For each sample, each individual amino acid $\delta^{13}C$ value was multiplied by the relative carbon molar concentration of that amino acid. The sum of these values is *w*AA $\delta^{13}C$, the weighted mean of amino acid $\delta^{13}C$ values. In addition, isotopic values of individual amino acids relative to total amino acid $\delta^{13}C$ were obtained by subtracting the absolute $\delta^{13}C$ value of each individual amino acid from the weighted mean value (*w*AA $\delta^{13}C$) to show the relative changes among individual amino acids. These will be referred to as "relative individual amino acid $\delta^{13}C$ values".

2.5. Statistical analysis

A degradation index (DI) calculation and a linear discriminant function analysis (Larsen et al., 2013) were applied to the data using the relative abundance (mol%) and relative individual amino acid $\delta^{13}C$ values measured in both particles and surface sediments of the Pearl River estuary (see Supplementary Materials).

2.6. Lability Model development and assumptions

To better differentiate between the diverse estuarine organic carbon sources, we developed a Lability Model with the following assumptions about composition and isotopic values:

(1) Composition: We assumed that particulate organic matter (POM) in the Pearl River estuary originates either from algal production or from terrestrial input. For our purposes, algal derived organic carbon is made up of labile algal material (LabiAM), e.g., amino acids, and semi-labile algal material (SemiAM), e.g., AIF and lipids. Other cellular components, e.g., carbohydrates, amino sugars, etc., account for less than 10% of total algal organic carbon (Whitehead et al., 2008), and are thus ignored in the model. We assumed that amino acids are produced only as LabiAM and that LabiAM is subject to degradative changes during transport in the estuary. To make a solution possible, we assumed that terrestrial organic matter (TerrOM) comes only from soil OM and experiences no degradative modification during its transport in the estuary (Yu et al., 2010). Other terrestrial inputs, e.g., woody tissues, account for a negligible contribution to estuarine POC in this region (Zhang et al., 2014). The contribution of macrophytes and benthos were also assumed to be negligible since the samples were collected from the surface water of the estuary with faster discharge.

(2) Isotopic signature: We assumed that the isotopic value of LabiAM is the mean of the $\delta^{13}C$ values of total amino acids (*w*AA $\delta^{13}C$) measured in this study. In our model, lipids and AIF (SemiAM) are assumed to share the same isotopic signature, which is 4.53‰ lower than amino acids from the same algal source. This assumption for $\delta^{13}C$ difference between SemiAM and LabiAM (Δ) was based on the average isotopic difference between amino acids and AIF identified in sinking particles from the Equatorial Pacific (-4.53 ± 0.48‰, $n = 14$) by Hwang and Druffel (2003). During decomposition, a progressive decrease in relative abundance of LabiAM concentration is accompanied by a relative increase in SemiAM, with both retaining their characteristic $\delta^{13}C$ values (Wang et al., 1998). It then follows the mass balance that the $\delta^{13}C$ values of algal organic carbon depends on the relative abundance and $\delta^{13}C$ values of the two parts. Thus the ratio f_{LabiAM}/f_{SemiAM} generally reflects the change in lability of algal organic matter. We assume that terrigenous organic matter from soil OM (TerrOM) has an isotopic value ($\delta^{13}C_{TerrOM}$) of -24.1 ± 1.0‰ as reported for Pearl River estuary riverbank sediment (Yu et al., 2010).

With these assumptions, our model used the measured trends in relative distribution and $\delta^{13}C$ value of LabiAM, SemiAM and TerrOM throughout the estuary to describe the concomitant trends in major carbon inputs. To summarize, we divided estuarine POC as follows: 1) LabiAM with its $\delta^{13}C$ value being the *w*AA $\delta^{13}C$ calculated from data presented here; 2) SemiAM with $\delta^{13}C_{SemiAM}$ of 4.53‰ lower than LabiAM; 3) TerrOM with $\delta^{13}C_{TerrOM}$ of -24.1‰. With the identification of *w*AA $\delta^{13}C$, the carbon isotope values of LabiAM, SemiAM and TerrOM can be predicted for each particulate sample. Based on mass and carbon isotope balances, the following two equations can be established:

$$\delta_{POC} = f_{LabiAM} \times \delta_{LabiAM} + f_{SemiAM} \times \delta_{SemiAM} + f_{TerrOM} \times \delta_{TerrOM} \quad (1)$$

$$1 = f_{LabiAM} + f_{SemiAM} + f_{TerrOM} \quad (2)$$

where f_{LabiAM}, f_{SemiAM} and f_{TerrOM} are percentages of the three groups relative to POC. The value of f_{LabiAM} can be obtained from AA carbon yields. In this way, the relative contributions of the rest two groups of POM can be calculated. Then, the concentrations of organic carbon from the three groups can be quantified by multiplying POC concentrations by the three percentages (f_{LabiAM}, f_{SemiAM} and f_{TerrOM}). Error propagation of the above two equations is described in the Supplementary Materials S1.4.

3. RESULTS

3.1. Hydrology and geochemistry of Pearl River estuary

The nitrate concentrations in Pearl River estuary decreased rapidly along the surveyed salinity transect, from 389 μmol/L to values below our detection level (Fig. 2). Total suspended materials (TSM) showed a significant increase in areas with intermediate salinity values (A01, A04, Fig. 2), although it was not directly associated with the turbidity maximum. The highest concentrations of Chl*a* (P03, P04) were at the upper end of the estuary. These high concentrations were gradually diluted with distance downstream. A small peak in Chl*a* was also observed at the saline end near Sta. A08 where lower TSM favors the growth of phytoplankton.

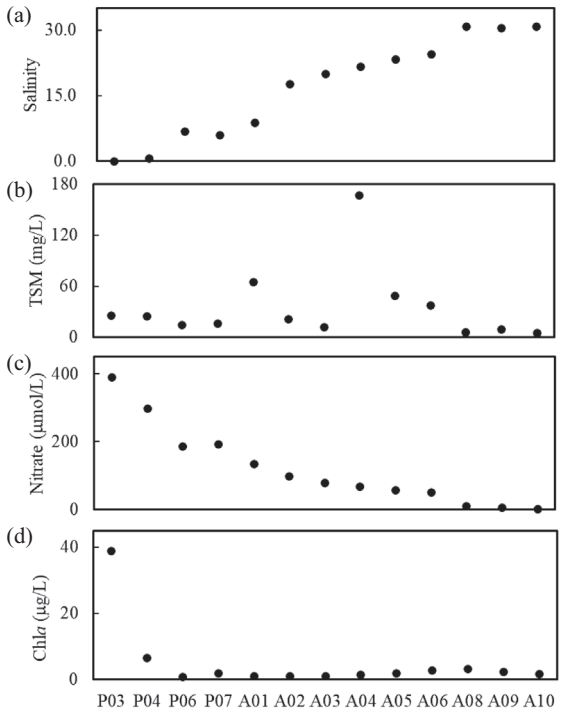

Fig. 2. Distribution of salinity, total suspended matter, nitrate and Chl*a* concentrations in surface water along the Pearl River Estuary.

3.2. Distribution of amino acids and bulk organic carbon $\delta^{13}C$ values

Amino acid $\delta^{13}C$ values were measured in surface suspended particles collected along the transect and ranged from −36.1‰ to −9.8‰ (Fig. 3a, Table S2). Large differences in isotope ratios were observed among individual amino acids in the same samples, with leucine and valine as the most isotopically depleted AA and glycine and threonine as the most enriched AA in C^{13}. Similar patterns were observed in surface sediments (Fig. 3c, Table S1), suggesting that suspended particles and surface sediments share a similar amino acid source and diagenetic pathway.

Relative individual amino acid $\delta^{13}C$ values were then compared across stations by subtracting each individual amino acid $\delta^{13}C$ from *w*AA $\delta^{13}C$ (Fig. 3b, d), where *w*AA $\delta^{13}C$ is the weighted mean of all ten amino acid $\delta^{13}C$ values measured in the sample. These are referred to as relative individual amino acid $\delta^{13}C$ values. Val and Thr in suspended particles showed the largest variations in relative AA $\delta^{13}C$ among stations, up to 9.6‰ for Val and 12.6‰ for Thr, while Leu and Glu (including glutamine) $\delta^{13}C$ values had the least variation throughout the stations surveyed, 1.7‰ and 2.7‰, respectively. A slightly different response was observed in surface sediments, with the largest relative $\delta^{13}C$ variation in Gly and Thr, and the smallest in Asp and Glu. The differences in relative amino acid $\delta^{13}C$ values suggests that amino acid isotope fractionations are not uniformly generated and altered during their transport through the estuary.

Although OC and AA concentrations in both particles and sediments showed no clear pattern with salinity (Fig. 4a, b), there was a general increase in *w*AA $\delta^{13}C$ and $\delta^{13}C$ values of bulk organic carbon in samples from the river end to the mouth of the estuary (Fig. 4c, d). This increase in $\delta^{13}C$ ranged from −29.2‰ to −18.3‰ for particulate amino acids and from −29.0‰ to −19.1‰ for POC. Amino acids were slightly enriched in ^{13}C relative to bulk organic carbon, and the isotopic difference between amino acids and POC across the stations was in the range of −1.2‰ to 2.8‰. Amino acids in surface sediments were also elevated in $\delta^{13}C$, ranging from −21.5‰ to −15.8‰. This isotopic range is smaller than that in the suspended particles (Fig. 4c, d). This smaller isotope range in surface sediments results from a much higher *w*AA $\delta^{13}C$ in river-end sediment of −21.5‰ compared to the −29.2‰ value in the freshwater particles, but a smaller difference in *w*AA $\delta^{13}C$ values between suspended particles and sediment from saline stations. Meanwhile, the $\delta^{13}C$ of bulk organic carbon in surface sediments (SOC) was rather constant at about −25‰ upstream, but was slightly higher at the more saline stations, about −22‰ (Fig. 4d). This results in a larger difference in $\delta^{13}C$ of up to 6.0‰ between amino acids and bulk organic carbon in sediment compared to the isotopic difference (−1.2‰ to 2.8‰) found in suspended particles.

3.3. Model results describing sources and lability of POM

LabiAM usually accounts for a small portion of POC (Fig. 5b). Exceptions are at Sta. P07 and A02, where LabiAM accounts for up to 64% of the POM. SemiAM is a major component of estuarine POM, ranging from 4.6 μmolC L^{-1} to 38.6 μmolC L^{-1} across the transect, and accounting for 18.7–81.1% of POM (Fig. 5b, c). The relative abundance of TerrOM (f_{TerrOM}), calculated using Eqs. (1) and (2), show considerable variation, ranging from 16.9% to 77.4% (Fig. 5b). This is equivalent to a terrestrial input of up to 48.9 μmolC L^{-1} at A04 (Fig. 5c). Stations with higher TerrOM input (Sta. A01 and A04) contain higher loadings of TSM (Fig. 2c, 5b, 5c). These higher TSM stations also have lower f_{LabiAM} values (Fig. 5b). The ratio of f_{LabiAM} over f_{SemiAM} can be considered as an indicator of lability of algal OM (Fig. 5d). A ratio of f_{LabiAM}/f_{SemiAM} from 0.14 to 3.44 was observed but only two stations were greater than 1 (Sta. P07 and A02), which indicates a dominance of freshly produced OM there.

The model failed to predict f_{TerrOM} at the lower reaches of the estuary (A06, A08 and A10) because predicted $\delta^{13}C$ values for SemiAM and TerrOM are so close to each other (Fig. 5b) at these saline stations that Eqs. (1) and (2) could not distinguish between f_{SemiAM} and f_{TerrOM} as suggested by error propagation (Table S8). For this reason, terrestrial input is potentially underestimated at these stations. To evaluate the potential influence of the presumed offset Δ, an uncertainty of 15% was considered as the upper limit of Δ, which results in up to a five time increase in the uncertainty of f_{SemiAM} (Table S8). Consequently, the model can only be applied at upstream stations like P04 and A01.

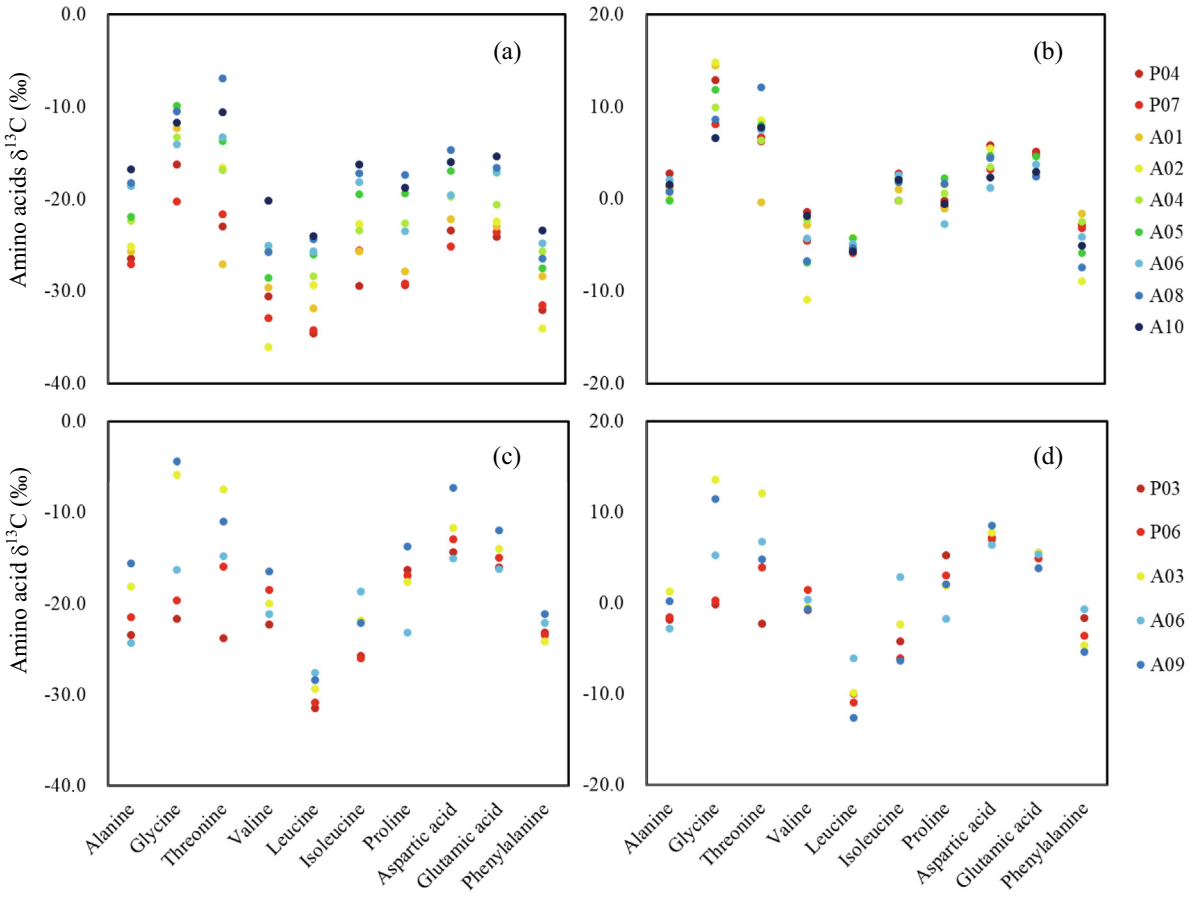

Fig. 3. The distribution of $\delta^{13}C$ values of amino acids in suspended particles in surface water and surface sediment along the transect: (a) the $\delta^{13}C$ values of amino acids in suspended particles; (b) the $\delta^{13}C$ values of particulate amino acid relative to *w*AA$\delta^{13}C$; (c) the $\delta^{13}C$ values of amino acid of surface sediment; and (d) the $\delta^{13}C$ values of sedimentary amino acid relative to *w*AA $\delta^{13}C$.

4. DISCUSSION

4.1. Contribution of algal OM to the estuarine POM

(1) Labile algal material

Values of $\delta^{13}C$ in both amino acids and bulk organic carbon in suspended particles increase from upstream stations to ocean stations (Fig. 4c). In spite of tidal and seasonal variations expected to influence this distribution, this gradient in amino acid $\delta^{13}C$ is consistent with "phytoplankton" $\delta^{13}C$ values predicted from dissolved inorganic carbon $\delta^{13}C$ observed in the Pearl River estuary during the dry season (−28‰ to −21‰, Guo et al., 2015; Zhao et al., 2020). This consistency in the carbon isotope distribution indicates that carbon fixation by phytoplankton is likely the dominant process causing the $\delta^{13}C$ gradients observed in amino acids along the estuary. In addition to changes in dissolved inorganic carbon isotopic values, a shift in isotope fractionation can potentially influence the gradients of *w*AA $\delta^{13}C$ caused by changing phytoplankton community, which responds to the changing growth rate, cell geometry and other physiological factors among species (Popp et al., 1998). Following up on this idea, a linear discriminant function analysis provides evidence that microalgae and bacteria are the dominant sources of particulate amino acids in the Pearl River estuary compared to seagrasses and terrestrial plants (Figs. S3, S4).

Similar carbon isotope gradients between fresh and saline waters have been observed in particulate lipids and Chl*a* from Gulf of Mexico estuaries, where $\delta^{13}C$ values in the total lipid extract and chlorophyll ranged from −31‰ to −20‰, and from −31‰ to −18‰, respectively, compared to bulk organic carbon $\delta^{13}C$ values that ranged from −27‰ to −18‰ (Qian et al., 1996). These isotope gradients in labile organic compounds like amino acids, short-chain lipids and pigments imply that isotope values of freshly produced organic carbon along the salinity transect reflect both their inorganic carbon source and their fractionation during carbon fixation (McIntosh et al., 2015). The *w*AA $\delta^{13}C$ values observed in surface sediments show a similar increase with increasing salinity (Fig. 4d), but to a lesser extent (ranging from −21.5‰ to −15.8‰ in sediment *w*AA $\delta^{13}C$ compared to those in suspend particles ranging from −29.2‰ to −18.3‰, Fig. 4c, d). The smaller increase in

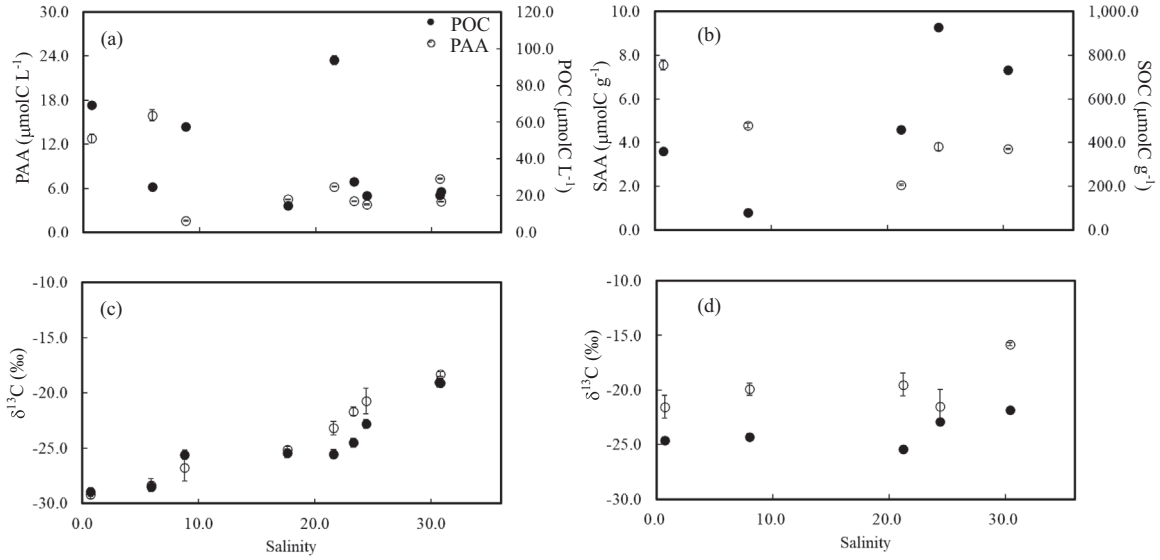

Fig. 4. Concentrations of amino acids (open circle) and bulk organic carbon (solid circle) in (a) suspended particles and (b) sediment, and weighted means of amino acid $\delta^{13}C$ (open circle) and bulk organic carbon $\delta^{13}C$ (solid circle) in the (c) suspended particle and (d) sediment samples. PAA: particulate amino acid; SAA: sediment amino acids. The scale bars of PAA and SAA concentrations (n = 3) are on the left y-axes, and those of POC and SOC concentrations are on the right y-axes.

sediment *w*AA $\delta^{13}C$ relative to suspended particles may result either from salt water intrusion in the deep water or from somewhat longer residence times of amino acids in surface sediments (Dai et al., 2014; Lin et al., 2019).

Algal amino acids are subject to rapid remineralization and molecular alteration in aquatic environments. The carbon isotope values of amino acids observed in the estuary are in good agreement with that seen in particles collected from the open ocean and from the Columbia River (Keil and Fogel, 2001; McCarthy et al., 2004; Hannides et al., 2013). The $\delta^{13}C$ values of individual amino acids are a net result of both autotrophic production and degradative alteration, which are driven by either heterotrophic bacterial reworking or zooplankton grazing. Wang et al. (1998) found that $\delta^{13}C$ values of bulk hydrolyzable amino acids in sinking particles were constant with depth from the surface water to the sediment, indicating that the characteristic amino acid isotopic signature from primary production and decomposition in the surface water experienced little change during sinking in the water column. This is supported by our finding that the relative $\delta^{13}C$ values of individual amino acid had less variation among stations (Fig. 3b, d), although *w*AA $\delta^{13}C$ increased due to the $\delta^{13}C$ changes in dissolved inorganic carbon.

(2) Semi-labile algal material

In the Lability Model, both lipids and AIF are assumed to be included in SemiAM since they share the same isotopic signature (Hwang and Druffel, 2003). In phytoplankton cells, most SemiAM is in the form of lipids. It has been reported that lipids usually account for less than 10% of the cellular carbon (Whitehead et al., 2008). In decomposed organic matter, more SemiAM is in the form of AIF, which is more refractory against further degradation (Wang et al., 1998; Hwang et al., 2006; Wakeham and Lee, 2019). Regardless of how fresh or refractory the SemiAM is, we assume that LabiAM and SemiAM account for most of the organic carbon in marine particles: for example, these two components account for about 40–70% of phytoplankton, 85% in zooplankton and more than 80% of total OC in sinking particles from the Equatorial Pacific and suspended particles from the continental shelf (Wakeham et al., 1997; Wang et al., 1998; Chen et al., 2004). Other compounds, like carbohydrates and amino sugars, make a lesser contribution to POC. Therefore, the relative abundance (f_{LabiAM}, f_{SemiAM}) and isotopic values (δ_{LabiAM}, δ_{SemiAM}) of LabiAM and SemiAM determine the $\delta^{13}C$ values of most of the particulate organic carbon. In the open ocean, a rather constant carbon isotope difference of 4.53‰ has been observed between LabiAM and SemiAM in sinking particles (calculated from Fig. 3 in Hwang and Druffel, 2003). Isotope differences among organic classes are widely observed, and depend on the metabolic pathways by which the molecules are synthesized (Hayes, 2001 and reference therein). A rather consistent depletion in lipid ^{13}C has been predicted globally relative to the total biomass of natural populations of phytoplankton (−3.5‰ to −4.5‰, Hayes, 2001), suggesting a relatively constant isotope difference among major classes of organic compounds across diverse marine environments.

However, unlike the open ocean where most organic matter is produced by phytoplankton in surface waters (e.g., Wang et al., 1998; Roland et al., 2008), coastal organic matter originates from more diverse sources (e.g., Hedges and Keil, 1999; Canuel, 2001). Chen et al. (2008) measured the $\delta^{13}C$ values of amino acid, lipid and AIF fractions isolated from suspended particles and sediments on

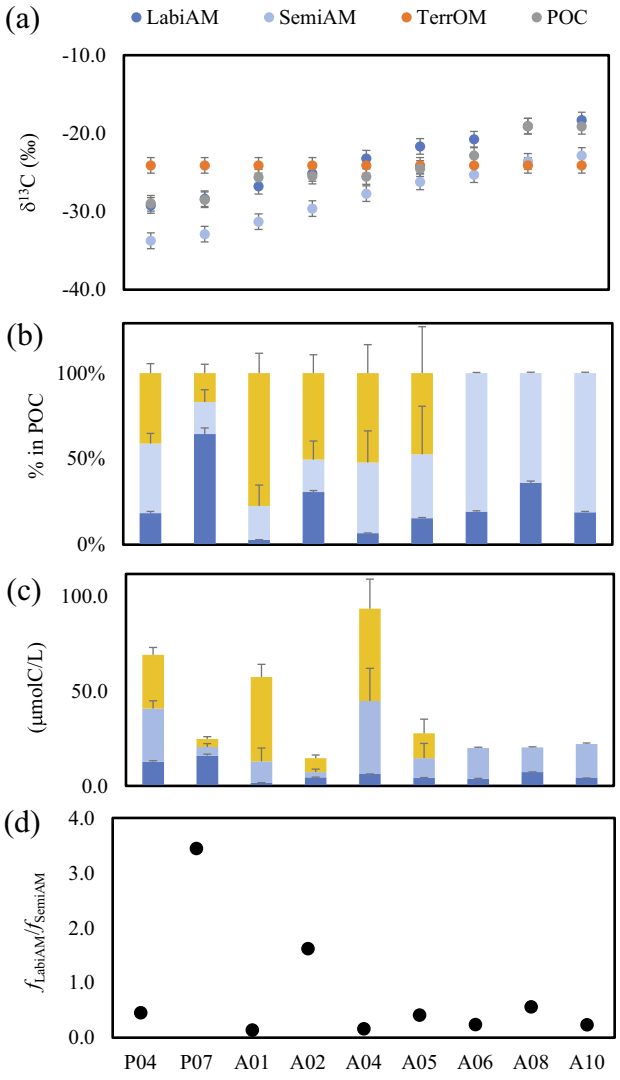

Fig. 5. Source and lability of Pearl River estuary suspended particles as calculated from the Lability Model: (a) measured $\delta^{13}C$ values of LabiAM, and presumed $\delta^{13}C$ values of SemiAM and TerrOM in the Lability Model for suspended particles; (b) relative abundance of LabiAM, SemiAM and TerrOM in POC as calculated by the Lability Model; (c) concentrations of LabiAM, SemiAM and TerrOM as calculated by the Lability Model; and (d) lability of algal derived OM as indicated by the ratio of f_{LabiAM} to f_{SemiAM}. The error bars of LabiAM (n = 3) are the standard deviation of measurement, and the error bars of SemiAM and TerrOM are their standard deviations as calculated by error propagation using the Lability Model (as in the supplementary materials S1.4).

the shelf adjacent to the Pearl River estuary. Particulate $\delta^{13}C$ values varied among the amino acids (−20.7‰), lipids (−26.1‰) and AIF (−24.9‰). This observation appears to contradict our assumption of isotopic similarity between lipid and AIF fractions. Since a major portion of terrestrial OM may be in the form of AIF, the observation that AIF is isotopically heavier than lipids in the shelf particles could result from the contribution of terrestrial OM when using a direct measurement of the bulk fractions. Therefore, a direct investigation of OM chemical fractions cannot separate OM from diverse estuarine OM sources (Roland et al., 2008). However, the shift in estuarine AIF does not influence our model, which sorts OM based on isotopic signature. The SemiAM in our model only considers AIF from algal production, which has a constant isotopic linkage with LabiAM, while AIF from terrestrial OM is included in TerrOM. Considering this, the changing terrestrial input only influences the f of the three fractions, but not their $\delta^{13}C$ values.

Application of the Lability Model showed a major contribution of SemiAM in the estuarine POC (Fig. 5b, c). The contribution of SemiAM was usually larger than LabiAM except at Station P07 and A02 (Fig. 5b). The sum of algal LabiAM and SemiAM usually accounts for about half of the POM in most stations (with only one exception, 22.6% at Sta. A01), indicating a dominance of algal OM to the estuarine OM. However, the variation in f_{LabiAM}/f_{SemiAM} ratio along the salinity transect (Fig. 5d) suggests

that the lability of algal OM varies significantly, probably as a result of the balance between prevailing production and degradation processes during its transport across the estuary. The elevated f_{LabiAM}/f_{SemiAM} ratio in the upstream stations may result from higher phytoplankton growth as a response to elevated nutrient inputs, as is frequently observed in the upper reaches of the Pearl River estuary (He et al., 2010b). In the middle stations, high turbidity inhibits phytoplankton growth but decomposition continues. Even though the Lability Model cannot separate SemiAM from TerrOM at downstream stations, A06, A08 and A10, SemiAM should still be the major OM component considering the limited influence from sediment resuspension and terrestrial input downstream.

(3) Terrestrial organic carbon

Terrestrial organic matter originating from vascular plant and soil OM is dominated by refractory components, like lignin and carbohydrates from vascular plants, and humic substances from soil (Benner et al., 1987; Bianchi, 2011; Whitehead et al., 2008). Thus terrestrial organic matter can have a much longer residence time than algal organic matter (Benner et al., 1987), and thus neither the molecular composition nor the isotope signature of terrestrial POC are subject to major change during transport through the estuary. This is likely why we observed little change in bulk $\delta^{13}C$ values in upstream surface sediment, and why the TerrOM $\delta^{13}C$ value of −24.1‰ was applied uniformly in the model for terrestrial organic carbon in the estuary from soil OM (Yu et al., 2010). Results from the Lability Model suggest a dominant but highly variable TerrOM contribution to surface suspended particles for the Pearl River estuary (Fig. 5b); this contribution was usually higher than that of SemiAM, with the highest contribution at stations A01 and P04 where higher TSM input was also observed (Fig. 2c). Higher values of both f_{TerrOM} and TSM at A01 and P04 in suspended particles suggest that terrestrial input originates from local resuspension of sediment or lateral transported OM along the watershed, rather than input from river discharge; otherwise, a decrease of f_{TerrOM} would be observed downstream.

However, several processes can alter TerrOM composition, such as selective aggregation/coagulation of certain compounds during the mixing of river and saline water masses, production of macrophytic and benthic OM, resuspension of highly degraded sediment OM, the input from the adjacent mangrove and marsh (Bianchi and Bauer, 2011), as well as photooxidation of terrestrial OM (Ward et al., 2013, 2015). The potential influence of these processes on TerrOM $\delta^{13}C$ is poorly constrained in the estuary. Another challenge for our model is to evaluate the influence of anthropogenic inputs. Heavy loadings of nutrients and anthropogenic organic matter may enter the estuary in sewage from adjacent urban areas (He et al., 2014). We found higher amino acid concentrations in the upper reaches of the estuary (Fig. 4a), where the largest metropolitan areas in southern China are found. However, it is hard to differentiate the sources of these amino acids, whether they came directly from anthropogenic sources, or resulted from algal growth in response to anthropogenic nutrient inputs. The latter may be more important to estuarine organic carbon, because *w*AA $\delta^{13}C$ values at the upper reaches of the estuary are consistent with *in situ* algal production from local dissolved inorganic carbon, rather than from sewage input, which has $\delta^{13}C$ values of bulk organic carbon ranging from −22.9‰ to −28.0‰ (Rumolo et al., 2011, and references therein). Thus, amino acids produced due to anthropogenic nutrient inputs might best be included in algal-derived organic carbon.

Taken together, these evidences demonstrate that TerrOM plays an important role in the estuarine POC flux, and that TerrOM distributions are influenced by local resuspension of sedimentary OM and/or laterally transported OM along the watershed. The influences of seasonal variations, storm events, and other process may be underestimated in our study due to the limited temporal resolution of sampling.

4.2. Implications and limitations of the Lability Model

This preliminary study of amino acid $\delta^{13}C$ distribution in the Pearl River estuary provides us with new insights into estuarine OM and its contribution to the ocean carbon cycling. First, algal OM is subject to rapid changes in molecular composition and isotope values during its transport in the estuary. These rapid changes make it particularly challenging to quantitatively evaluate algal OM contributions to estuarine POM. Two common strategies have been widely applied to assess this problem: (1) quantifying algal OM abundance using an algal-specific biomarker as a proxy (Bianchi and Canuel, 2011 and references therein), and (2) differentiating algal OM from other sources by its characteristic isotope value (Peterson and Fry, 1987). The former strategy assumes a constant relative abundance of biomarker to algal OM even during decomposition. The latter strategy assumes that algal OM produced in the estuary has an isotope value that remains the same throughout the estuary regardless of degradative modifications (Hedges et al., 1997). Both assumptions run into problems in estuaries where dynamic production and degradation processes affect labile organic matter. Instead, the Lability Model simulates the changing molecular composition and isotope values of algal OM during decomposition. This approach circumvents the isotope shift in bulk organic carbon that occurs during degradation and provides a more precise evaluation of algal OM distribution (both labile and semi-labile) in the estuary. This model is particularly useful in ecosystems where highly dynamic hydrological and geochemical gradients limit a precise quantification of organic carbon from different sources.

Secondly, the fate of estuarine OM in the ocean is largely determined by its lability and its flux to the ocean. It has been generally assumed that exported estuarine OM is dominated by more refractory terrestrial OM which has bypassed the estuary and buried in the coastal ocean (e.g., Cai, 2011). The major contribution of SemiAM in the Pearl River estuary indicates that algal OM in the estuary is preferentially in the form of semi-labile components like lipid

material and AIF. Thus, the autochthonous carbon produced by estuarine algae is not just remineralized locally (Canuel and Hardison, 2016), but a large portion of it has also been transformed into SemiAM and exported into the coastal ocean. Thus, we must reconsider the origin and fate of OM from estuaries in coastal ocean carbon budgets (Najjar et al., 2018). This process is potentially more and more important as higher contributions from algal production have been predicted for future estuaries due to increasing anthropogenic activities (Canuel and Hardison, 2016).

In future applications of the Lability Model, its limitations must be better evaluated. This model separates algal OM into LabiAM and SemiAM according to their distinctive lability and isotopic signatures (Wang et al., 1998; Hwang and Druffel, 2003). It assumes that LabiAM and SemiAM have constant isotopic values once they are produced, but that their relative abundances are subject to change during degradation. Thus, a reliable prediction from the Lability Model requires the following: First, the $\delta^{13}C$ values of compounds from individual sources must be distinguishable from each other. This is a major reason why the model failed to quantify TerrOM in the downstream stations where SemiAM and TerrOM show similar $\delta^{13}C$ values. This limits application of the Lability Model to environments where organic compounds from distinctive origins have overlapping ranges of isotope values. Second, the isotopic offset between LabiAM and SemiAM (Δ) must be well identified. Based on our uncertainty analysis, the model can only be applied to the uppermost stations when the offset Δ has an uncertainty of 15% (Supplementary materials S1.4, Table S8). This uncertainty may result from the changing isotope relationship among individual molecules which is originally determined by the diverse metabolisms of source organisms. The uncertainty could also result from the varied abundance of laterally transported LabiAM and SemiAM along the estuary due to the difference in their residence time. Uncertainty in the offset Δ can be largely constrained when both amino acid and algal lipid $\delta^{13}C$ values and concentrations are available. Third, the molecular composition and isotopic signature of recalcitrant terrestrial OM must remain constant during transport of the POM from one location to another. Alternatively, the $\delta^{13}C$ and concentration of terrestrial biomarkers like lignin could be incorporated into the model to better evaluate the TerrOM contribution.

Overall, this model demonstrates the potential of compound specific isotope studies to decipher both sources and transformations of particulate organic carbon in an estuary. It emphasizes the geochemical importance of better understanding the intrinsic isotopic relationship among individual molecules and the application of multiproxy in compound-specific isotope analysis. Our model, to the best of our knowledge, is one of the few that has considered the influence of molecular transformation during OC transport. This model could also be applied to other estuaries, e.g., the Amazon and Changjiang, to examine sources and transformation of algal organic carbon in those systems.

Declaration of Competing Interest

The authors declare that they have no known competing financial interests or personal relationships that could have appeared to influence the work reported in this paper.

ACKNOWLEDGEMENTS

We thank Junhui Chen, Yongyu Li, Baomin Liu, Jie Liu, Jing Su, Li Tian, Lai Wei and Xijie Yin for help with instrumentation. We also thank the captain and crew of R/V Haishun for their help during the sampling cruise. We very much appreciate the many valuable suggestions from the editor and four reviewers. This work was supported by the National Natural Science Foundation of China, China (No. 41703070, 41976035 and No. 41576085), a MEL Visiting Fellowship (Xiamen University, China) granted to Cindy Lee, and Fundamental Research Funds for the Central Universities, China (No. 20720160112).

APPENDIX A. SUPPLEMENTARY MATERIAL

Supplementary data to this article can be found online at https://doi.org/10.1016/j.gca.2020.11.010.

REFERENCES

Benner R., Fogel M., Sprague E. K. and Hodson R. E. (1987) Depletion of ^{13}C in lignin and its implications for stable carbon isotope studies. *Nature* **329**, 708–710.

Bianchi T. S. and Bauer J. E. (2011) Particulate organic carbon cycling and transformation. *Treatise Estuarine Coast. Sci.* **5**, 67–117.

Bianchi T. S. (2011) The role of terrestrially derived organic carbon in the coastal ocean: A changing paradigm and the priming effect. *Proc. Natl. Acad. Sci. USA* **108**, 19473–19481.

Bianchi T. S. and Canuel E. A. (2011) *Chemical Biomarkers in aquatic ecosystems*. Princeton Univ. Press, Princeton, NJ.

Cai W.-J. (2011) Estuarine and Coastal Ocean Carbon Paradox: CO2 Sinks or Sites of Terrestrial Carbon Incineration? Available at: *Ann. Rev. Mar. Sci.* **3**, 123–145 http://www.annualreviews.org/doi/10.1146/annurev-marine-120709-142723.

Canuel E. A., Cloern J. E., Ringelberg D. B., Guckert J. B. and Rau G. H. (1995) Molecular and isotopic tracers used to examine sources of organic matter and its incorporation into the food webs of San Francisco Bay. *Limnol. Oceanogr.* **40**, 67–81.

Canuel E. A. (2001) Relations between river flow, primary production and fatty acid composition of particulate organic matter in San Francisco and Chesapeake bays: A multivariate approach. *Org Geochem.* **32**, 563–583.

Canuel E. A. and Hardison A. K. (2016) Sources, ages, and alteration of organic matter in Estuaries. *Ann. Rev. Mar. Sci.* **8**, 409–434.

Chen F., Zhang L., Yang Y. and Zhang D. (2008) Chemical and isotopic alteration of organic matter during early diagenesis: Evidence from the coastal area off-shore the Pearl River estuary, south China. *J. Mar. Syst.* **74**, 372–380.

Chen J., Li Y., Yin K. and Jin H. (2004) Amino acids in the Pearl River Estuary and adjacent waters: Origins, transformation and degradation. *Cont. Shelf Res.* **24**, 1877–1894.

Cloern J. E., Canuel E. A. and Harris D. (2002) Stable carbon and nitrogen isotope composition of aquatic and terrestrial plants of

the San Francisco Bay estuarine system. *Limnol. Oceanogr.* **47**, 713–729.
Close H. G. (2019) Compound-Specific Isotope Geochemistry in the Ocean. *Ann. Rev. Mar. Sci.* **11**, 10.1–10.30.
Dai S. B., Yang S. L. and Cai A. M. (2008a) Impacts of dams on the sediment flux of the Pearl River, southern China. *Catena* **76**, 36–43.
Dai M., Wang L., Guo X., Zhai W., Li Q., He B. and Kao S.-J. (2008b) Nitrification and inorganic nitrogen distribution in a large perturbed river/estuarine system: the Pearl River Estuary, China. *Biogeosciences* **5**, 1227–1244.
Dai M., Gan J., Han A., Kung H. S. and Yin Z. (2014) Physical dynamics and biogeochemistry of the Pearl River plume. In *Biogeochemical Dynamics at Major River-Coastal Interfaces Linkages with Global Change* (eds. T. Bianchi, M. Allison and W.-J. Cai). Cambridge Univ. Press, New York, NY, USA, pp. 321–352.
Degens E. T., Behrendt M., Gotthardt B. and Reppmann E. (1968) Metabolic fractionation of carbon isotopes in marine plankton-II. Data on samples collected off the coasts of Peru and Ecuador. *Deep. Res. Oceanogr.* **15**, 11–20.
DeNiro M. J. and Epstein S. (1977) Mechanism of carbon isotope fractionation associated with lipid synthesis. *Science* **197**, 261–263.
Gordon E. S. and Goni M. A. (2003) Sources and distribution of terrigenous organic matter delivered by the Atchafalaya River to sediments in the northern Gulf of Mexico. *Geochim. Cosmochim. Acta* **67**, 2359–2375.
Goñi M. A., Ruttenberg K. C. and Eglinton T. I. (1998) A reassessment of the sources and importance of land-derived organic matter in surface sediments from the Gulf of Mexico. *Geochim. Cosmochim. Acta* **62**, 3055–3075.
Guo W., Ye F., Xu S. and Jia G. (2015) Seasonal variation in sources and processing of particulate organic carbon in the Pearl River estuary, South China. *Estuar. Coast. Shelf Sci.* **167**, 540–548.
Hannides C. C. S., Popp B. N., Anela C. C. and Drazen J. C. (2013) Midwater zooplankton and suspended particle dynamics in the North Pacific Subtropical Gyre: A stable isotope perspective. *Limnol. Oceanogr.* **58**, 1931–1946.
Hayes J. M. (2001) Fractionation of carbon and hydrogen isotopes in biosynthetic processes. *Rev. Mineral. Geochem.* **43**, 225–277.
He B., Dai M., Huang W., Liu Q., Chen H. and Xu L. (2010a) Sources and accumulation of organic carbon in the Pearl River Estuary surface sediment as indicated by elemental, stable carbon isotopic, and carbohydrate compositions. *Biogeosciences* **7**, 3343–3362.
He B., Dai M., Zhai W., Wang L., Wang K., Chen J., Lin J., Han A. and Xu Y. (2010b) Distribution, degradation and dynamics of dissolved organic carbon and its major compound classes in the Pearl River estuary, China. *Mar. Chem.* **119**, 52–64.
He B., Dai M., Zhai W., Guo X. and Wang L. (2014) Hypoxia in the upper reaches of the Pearl River Estuary and its maintenance mechanisms: A synthesis based on multiple year observations during 2000–2008. *Mar. Chem.* **167**, 13–24. https://doi.org/10.1016/j.marchem.2014.07.003.
Hedges J. I., Keil R. G. and Benner R. (1997) What happens to terrestrial organic matter in the ocean? *Org. Geochem.* **27**, 195–212.
Hedges J. I. and Keil R. G. (1999) Organic geochemical perspectives on estuarine processes: Sorption reactions and consequences. *Mar. Chem.* **65**, 55–65.
Hedges J. I., Eglinton G., Hatcher P. G., Kirchman D. L., Arnosti C., Derenne S., Evershed R. P., Kögel-Knabner I., de Leeuw J. W., Littke R., Michaelis W. and Rullkötter J. (2000) The molecularly-uncharacterized component of nonliving organic matter in natural environments. *Org. Geochem.* **31**, 945–958.
Hwang J. and Druffel E. R. M. (2003) Lipid-like material as the source of the uncharacterized organic carbon in the ocean? *Science* **299**, 881–884.
Hwang J., Druffel E. R. M., Eglinton T. I. and Repeta D. J. (2006) Source(s) and cycling of the nonhydrolyzable organic fraction of oceanic particles. *Geochim. Cosmochim. Acta* **70**, 5162–5168.
Jeffrey A. W. A., Pflaum R. C., Brooks J. M. and Sackett W. M. (1983) Vertical trends in particulate organic carbon 13C:12C ratios in the upper water column. *Deep Sea Res. Part A. Oceanogr. Res. Pap.* **30**, 971–983.
Kao S. J., Terence Yang J. Y., Liu K. K., Dai M., Chou W. C., Lin H. L. and Ren H. (2012) Isotope constraints on particulate nitrogen source and dynamics in the upper water column of the oligotrophic South China Sea. *Glob. Biogeochem. Cycles* **26**, 1–15.
Keil R. G. and Fogel L. (2001) Reworking of amino acid in marine sediments: coast amino acids in sediments along the Washington. *Limnol. Oceanogr.* **46**, 14–23.
Larsen T., Taylor D. L., Leigh M. B. and O'Brien D. M. (2009) Stable isotope fingerprinting: a novel method for identifying plant, fungal, or bacterial origins of amino acids Available at:. *Ecology* **90**, 3526–3535 http://www.ncbi.nlm.nih.gov/pubmed/20120819.
Larsen T., Wooller M. J., Fogel M. L. and O'Brien D. M. (2012) Can amino acid carbon isotope ratios distinguish primary producers in a mangrove ecosystem? Available at: *Rapid Commun. Mass Spectrom.* **26**, 1541–1548 http://www.ncbi.nlm.nih.gov/pubmed/22638971.
Larsen T., Ventura M., Andersen N., O'Brien D. M., Piatkowski U. and McCarthy M. D. (2013) Tracing carbon sources through aquatic and terrestrial food webs using amino acid stable isotope fingerprinting. *PLoS ONE* **8** e73441.
Larsen T., Bach L. T., Salvatteci R., Wang Y. V., Andersen N., Ventura M. and McCarthy M. D. (2015) Assessing the potential of amino acid 13C patterns as a carbon source tracer in marine sediments: Effects of algal growth conditions and sedimentary diagenesis. *Biogeosciences* **12**, 4979–4992.
Li D., Yao P., Bianchi T. S., Zhang T., Zhao B., Pan H., Wang J. and Yu Z. (2014) Organic carbon cycling in sediments of the Changjiang Estuary and adjacent shelf: Implication for the influence of Three Gorges Dam. *J. Mar. Syst.* **139**, 409–419. https://doi.org/10.1016/j.jmarsys.2014.08.009.
Li X., Liu Z., Chen W., Wang L., He B., Wu K., Gu S. and Jiang P. (2018) Production and transformation of dissolved and particulate organic matter as indicated by amino acids in the Pearl River Estuary, China. *J. Geophys. Res. Biogeosci.* **123**, 1–15.
Lin B., Liu Z., Eglinton T. I., Kandasamy S., Blattmann T. M., Haghipour N. and de Lange G. J. (2019) Perspectives on provenance and alteration of suspended and sedimentary organic matter in the subtropical Pearl River system, South China. *Geochim. Cosmochim. Acta* **259**, 270–287. https://doi.org/10.1016/j.gca.2019.06.018.
Mannino A. and Harvey H. R. (1999) Lipid composition in particulate and dissolved organic matter in the Delaware Estuary: Sources and diagenetic patterns. *Geochim. Cosmochim. Acta* **63**, 2219–2235.
McCallister S. L., Bauer J. E. and Canuel E. A. (2006) Bioreactivity of estuarine dissolved organic matter: A combined geochemical and microbiological approach. *Limnol. Oceanogr.* **51**, 94–100.
McCarthy M. D., Benner R., Lee C., Hedges J. I. and Fogel M. L. (2004) Amino acid carbon isotopic fractionation patterns in oceanic dissolved organic matter: an unaltered photoautotrophic source for dissolved organic nitrogen in the ocean? *Mar. Chem.* **92**, 123–134.
McIntosh H. A., McNichol A. P., Xu L. and Canuel E. A. (2015) Source-age dynamics of estuarine particulate organic matter

using fatty acid $\delta^{13}C$ and $\Delta^{14}C$ composition. *Limnol. Oceanogr.* **60**, 611–628.

Najjar R. G., Herrmann M., Alexander R., Boyer E. W., Burdige D. J., Butman D., Cai W. J., Canuel E. A., Chen R. F., Friedrichs M. A. M., Feagin R. A., Griffith P. C., Hinson A. L., Holmquist J. R., Hu X., Kemp W. M., Kroeger K. D., Mannino A., McCallister S. L., McGillis W. R., Mulholland M. R., Pilskaln C. H., Salisbury J., Signorini S. R., St-Laurent P., Tian H., Tzortziou M., Vlahos P., Wang Z. A. and Zimmerman R. C. (2018) Carbon budget of tidal wetlands, estuaries, and shelf waters of eastern North America. *Global Biogeochem. Cycles* **32**, 389–416.

Peterson B. J. and Fry B. (1987) Stable isotopes in ecosystem studies. *Annu. Rev. Ecol. Syst.* **18**, 293–320.

Popp B. N., Laws E. A., Bidigare R. R., Dore J. E., Hanson K. L. and Wakeham S. G. (1998) Effect of phytoplankton cell geometry on carbon isotopic fractionation. *Geochim. Cosmochim. Acta* **62**, 69–77.

Qian Y., Kennicutt M. C., Svalberg J., Macko S. A., Bidigare R. R. and Walker J. (1996) Suspended particulate organic matter (SPOM) in Gulf of Mexico estuaries: Compound-specific isotope analysis and plant pigment compositions. *Org. Geochem.* **24**, 875–888.

Rau G. H., Takahashi T., Des Marais D. J., Repeta D. J. and Martin J. (1992) The relationship between δ13C of organic matter and [CO2(aq)] in ocean surface water: Data from a JGOFS site in the northeast Atlantic Ocean and a model. *Geochim. Cosmochim. Acta* **56**, 1413–1419.

Roland L. A., McCarthy M. D. and Guilderson T. (2008) Sources of molecularly uncharacterized organic carbon in sinking particles from three ocean basins: A coupled $\Delta^{14}C$ and $\delta^{13}C$ approach. *Mar. Chem.* **111**, 199–213.

Rumolo P., Barra M., Gherardi S., Marsella E. and Sprovieri M. (2011) Stable isotopes and C/N ratios in marine sediments as a tool for discriminating anthropogenic impact. *J. Environ. Monit.* **13**, 3399–3408.

Sabadel A. J. M., Van Oostende N., Ward B. B., Woodward E. M. S., Van Hale R. and Frew R. D. (2019) Characterization of particulate organic matter cycling during a summer North Atlantic phytoplankton bloom using amino acid C and N stable isotopes Available at:. *Mar. Chem.*, 103670.

Scott J. H., Brien D. M. O., Emerson D., Sun H., Mcdonald G. D., Salgado A. and Fogel M. L. (2006) An examination of the carbon isotope effects associated with amino acid biosynthesis Available at:. *Astrobiology* **6**, 867–880 http://www.ncbi.nlm.nih.gov/pubmed/17155886.

Silfer J. A., Engel M. H., Macko S. A. and Jumeau E. J. (1991) Stable carbon isotope analysis of amino acid enantiomers by conventional isotope ratio mass spectrometry and combined gas chromatography/isotope ratio mass spectrometry. *Anal. Chem.* **63**, 370–374.

Strickland J. D. H. and Parsons T. R. (1972) A practical handbook of seawater analysis. *Bull. Fish. Res. Bd. Can.* **167**, 310.

Tang T., Mohr W., Sattin S. R., Rogers D. R., Girguis P. R. and Pearson A. (2017) Geochemically distinct carbon isotope distributions in *Allochromatium vinosum* DSM 180^{T} grown photoautotrophically and photoheterotrophically. *Geobiology* **15**, 324–339.

Wakeham S. G., Lee C., Hedges J. I., Hernes P. J. and Peterson M. J. (1997) Molecular indicators of diagenetic status in marine organic matter. *Geochim. Cosmochim. Acta* **61**, 5363–5369.

Wakeham S. G. and Lee C. (2019) Limits of our knowledge, part 2: Selected frontiers in marine organic biogeochemistry. *Mar. Chem.* **212**, 16–46.

Wang X. C., Druffel E. R. M., Griffin S., Lee C. and Kashgarian M. (1998) Radiocarbon studies of organic compound classes in plankton and sediment of the northeastern Pacific Ocean. *Geochim. Cosmochim. Acta* **62**, 1365–1378.

Ward N. D., Keil R. G., Medeiros P. M., Brito D. C., Cunha A. C., Dittmar T. and Richey J. E. (2013) Degradation of terrestrially derived macromolecules in the Amazon River. *Nat. Geosci.* **6** (7), 530.

Ward N. D., Krusche A. V., Sawakuchi H. O., Brito D. C., Cunha A. C., Moura J. M. S. and Richey J. E. (2015) The compositional evolution of dissolved and particulate organic matter along the lower Amazon River—Óbidos to the ocean. *Mar. Chem.* **177**, 244–256.

Whitehead K., Emerson S. R. and Hedges J. I. (2008) Marine organic geochemistry. In *Chemical Oceanography and the Marine Carbon Cycle* (eds. S. R. Emerson and J. I. Hedges), 1st ed. Cambridge Univ. Press, Cambridge, UK, pp. 262–302.

Wilkes E. B., Carter S. J. and Pearson A. (2017) CO2 -dependent carbon isotope fractionation in the dinoflagellate Alexandrium tamarense. *Geochim. Cosmochim. Acta* **212**, 48–61. https://doi.org/10.1016/j.gca.2017.05.037.

Wilkes E. B., Lee R. B. Y., McClelland H. L. O., Rickaby R. E. M. and Pearson A. (2018) Carbon isotope ratios of coccolith-associated polysaccharides of Emiliania huxleyi as a function of growth rate and CO2 concentration. *Org. Geochem.* **119**, 1–10. https://doi.org/10.1016/j.orggeochem.2018.02.006.

Yao P., Yu Z., Bianchi T. S., Guo Z., Zhao M., Knappy C. S., Keely B. J., Zhao B., Zhang T., Pan H., Wang J. and Li D. (2015) A multiproxy analysis of sedimentary organic carbon in the Changjiang Estuary and adjacent shelf. *J. Geophys. Res. Biogeosci.* **120**, 1407–1429. https://doi.org/10.1002/2014JG002831.

Yu F., Zong Y., Lloyd J. M., Huang G., Leng M. J., Kendrick C., Lamb A. L. and Yim W. W. (2010) Bulk organic $\delta^{13}C$ and C/N as indicators for sediment sources in the Pearl River delta and estuary, southern China. *Estuar. Coast. Shelf Sci.* **87**, 618–630.

Zhang S. R., Lu X. X., Higgitt D. L., Chen C. A., Han J. T. and Sun H. G. (2008) Recent changes of water discharge and sediment load in the Zhujiang (Pearl River) basin, China. *Glob. Planet. Change* **60**, 365–380.

Zhang Y., Kaiser K., Li L., Zhang D., Ran Y. and Benner R. (2014) Sources, distributions, and early diagenesis of sedimentary organic matter in the Pearl River region of the South China Sea. *Mar. Chem.* **158**, 39–48.

Zhao Y., Liu J., Uthaipan K., Song X., Xu Y., He B., Liu H., Gan J. and Dai M. (2020) Dynamics of inorganic carbon and pH in a large subtropical continental shelf system: Interaction between eutrophication, hypoxia, and ocean acidification. *Limnol. Oceanogr.* **65**, 1359–1379. Available at: https://onlinelibrary.wiley.com/doi/abs/10.1002/lno.11393.

Associate editor: Elizabeth Ann Canuel